



# Synthesis of polymer-supported Fe<sub>3</sub>O<sub>4</sub> nanoparticles and their application as a novel route for the synthesis of imidazole derivatives

Zeinab Hamidi<sup>1</sup> · Mohammad Ali Karimi Zarchi<sup>1</sup>

Received: 26 May 2018 / Accepted: 12 July 2018  
© Springer Nature B.V. 2018

## Abstract

Cross-linked poly(4-vinylpyridine) supported Fe<sub>3</sub>O<sub>4</sub> nanoparticles, abbreviated as [P<sub>4</sub>-VP]-Fe<sub>3</sub>O<sub>4</sub>NPs, were easily prepared as a new magnetic polymeric catalyst and efficiently used for the synthesis of imidazole derivatives. The polymeric catalyst was characterized by using of various techniques including field emission scanning electron microscopy, X-ray diffraction, vibrating sample magnetometry and Fourier transform infrared spectroscopy (FT-IR) techniques. According to the obtained results, good dispersion of Fe<sub>3</sub>O<sub>4</sub> nanoparticles on the polymer-support and excellent magnetic property of the catalyst were achieved. Various methods have been reported for the synthesis of multi-substituted imidazoles by the reaction of benzil, aldehydes and amines or ammonium acetate in the presence of various catalysts. These methods have some disadvantages including long reaction times, non-reusability of the catalyst, polluted reaction conditions, effluent pollution, and low yields; therefore, we wish to report an efficient, fast, clean and green method for the synthesis of imidazole derivatives that has been developed by one-pot condensation reaction of benzil, ammonium acetate and aldehydes in the presence of [P<sub>4</sub>-VP]-Fe<sub>3</sub>O<sub>4</sub> nanoparticles. The catalyst displayed good catalytic activity when applied for the synthesis of imidazole derivatives. Various imidazole derivatives were prepared in high to excellent yields (68–99%) with short reaction time and high purity. The present procedure offers advantages such as short reaction time, simple reaction work-up, and the polymeric catalyst can be regenerated and reused several times without significant loss of its activity.

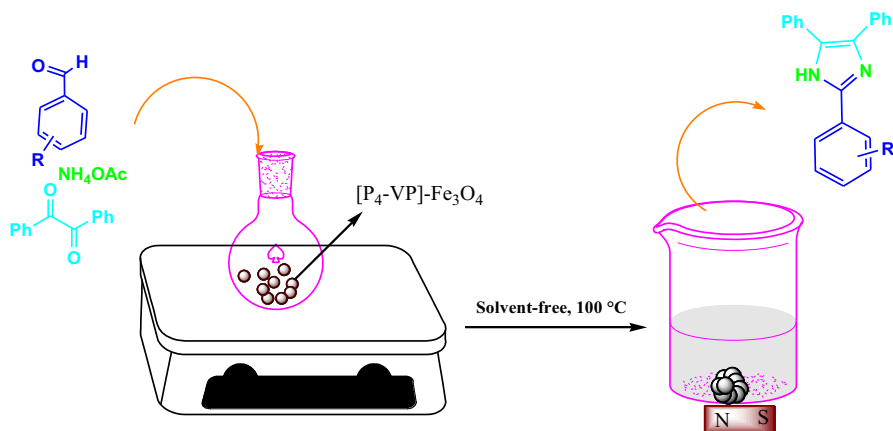
---

**Electronic supplementary material** The online version of this article (<https://doi.org/10.1007/s11164-018-3536-4>) contains supplementary material, which is available to authorized users.

---

Extended author information available on the last page of the article

## Graphical abstract



**Keywords** Imidazole synthesis · Magnetic nanoparticle · One-pot condensation reaction · Benzil · Polymeric catalyst

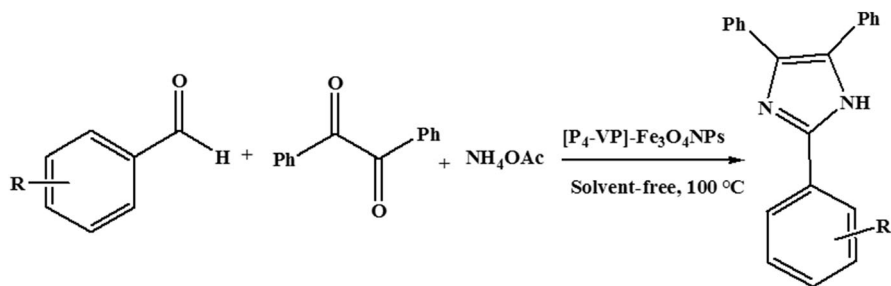
## Introduction

There are many studies that lately have reported on the preparation of nanoparticles because of their unrivaled physical and chemical properties compared to bulk materials. Recently, magnetic iron oxide nanoparticles (MNPs) have attracted much attention compared to other nanoparticles because of their unique physicochemical properties, great potential biomedical applications, large surface area, and fast response under applied external magnetic field, high coercivity and low Curie temperature [1–3]. Additionally, magnetically recyclable catalysts have the potential to approach catalysts benefiting from high activity, high selectivity, high stability, and easy separation, because MNP-immobilized catalysts combine the advantages of nanocatalysts with their inherent properties including non-toxicity, biocompatibility, facile assembling, and high accessibility of reusability through magnetic attraction [4, 5].  $\text{Fe}_3\text{O}_4$  have been applied in some new types of biomedical fields such as dynamic sealing [6], biosensors [7], contrast agents in magnetic resonance imaging [8], localizers in therapeutic hyperthermia [9] and magnetic targeted drug delivery systems [10]. Sun and Zeng reported, for the first time, simple organic-phase synthesis of magnetite nanoparticles with sizes variable from 3 to 20 nm in diameter [11]. Liz et al. employed water-in-oil microemulsion to obtain magnetic iron-oxide nanoparticles with size less than 10 nm [12–16]. However, these methods use organic solvents, which are not only higher cost, but also non-friendly to the environment, and is a major problem. Therefore, coprecipitation method, as an economic, biocompatible, and environmentally friend method, is usually used to synthesize MNPs [17, 18].

Polymeric reagents [19–22] and catalysts [23–25] have been extensively used in organic reactions for several years. The importance of these compounds compared to monomeric reagents result from their good properties such as insolubility in the reaction mixture, and thus their rapid and simple work-up, efficient reduction of the leaching of chemicals to reaction, solvent or environment at work-up procedures such as extraction or chromatography [26], safe handling, reusability of the reagents and reduction of environmental pollution in their presence because of their easy isolation by simple filtration. Therefore, by combining the positive properties of magnetic nanoparticles and polymeric reagents, we have a class of polymeric reagents and catalysts that show excellent magnetic properties.

Recently, imidazole derivatives have attracted considerable attention due to their biological properties including anti-allergenic, anti-inflammatory, analgesic, antifungal, antimycotic, antibiotic, antiulcerative, antibacterial and antitumor activities [27, 28]. They are also known as inhibitors of p38 MAP kinases and therapeutic agents [29]. Furthermore, substituted imidazole derivatives, especially tri- and tetra-substituted, act as plant growth regulators, glucagon receptors, photosensitive compounds in photography, and building blocks for the synthesis of other classes of compounds [30–32]. They have an important role in green chemistry as ionic liquids [33] and have optical absorption and bright luminescence [34]. Generally, in terms of physiological and pharmacological aspects, imidazoles are used to treat a variety of diseases [35]. According to these mentioned properties, synthesis of substituted imidazoles is still in demand. Debus reported for the first time in 1858 synthesized imidazole derivatives [36]. Over the years various methods have been reported for the synthesis of multi-substituted imidazoles by the reaction of benzil, aldehydes and amines or ammonium acetate in the presence of various catalysts such as ZnFe<sub>2</sub>O<sub>4</sub> [37], silica chloride [38], silica coated magnetic NiFe<sub>2</sub>O<sub>4</sub> nanoparticle-supported phosphomolybdic acid [39], copper nanoparticles [40], nano-copper and cobalt ferrites [41], FHS/SiO<sub>2</sub> [42], Fe<sub>3</sub>O<sub>4</sub> nanoparticles [43] and ZrCl<sub>4</sub> [44].

These methods have some disadvantages including long reaction time, non-reusability of the catalyst, polluted reaction condition, effluent pollution, and low yields; therefore, herein we aim to report an efficient, fast, clean and green method for the synthesis of trisubstituted imidazoles by one-pot three-component reaction of benzil, aldehydes and ammonium acetate in the presence of [P<sub>4</sub>-VP]-Fe<sub>3</sub>O<sub>4</sub> as a novel magnetic polymeric catalyst under solvent-free conditions (Scheme 1).



**Scheme 1** Synthesis of tri-substituted imidazoles by the one pot three-component reaction in the presence of [P<sub>4</sub>-VP]-Fe<sub>3</sub>O<sub>4</sub>

## Experimental

### Materials and instruments

All chemical materials and reagents were purchased from Fluka (Buchs, Switzerland), Aldrich (Milwaukee, WI, USA) and Merck (Germany) chemical companies with a purity of 99%. Polymeric reagent poly(4-vinylpyridine) cross-linked with 2% divinyl benzene, [P<sub>4</sub>-VP] 2% DVB, (white powder, 100–200 mesh, purity of 99%) and thin-layer chromatography (TLC) with silica gel PolyGram SIL G/UV 254 plates were purchased from Fluka. Characterization of all products was done by comparison of their melting points, Fourier transform infrared (FTIR) spectroscopy, and <sup>1</sup>H and <sup>13</sup>C-NMR spectral data with those of known products, and all yields refer to the isolated pure products. The melting points were determined with a Buchi melting point B-540 B. V.CHI apparatus. The FTIR spectra were obtained with a Bruker Equinox (model 55), Germany, and the NMR spectra were recorded on a Bruker AC 400 Avance DPX spectrophotometer, Germany at 400 MHz for <sup>1</sup>H and at 100 MHz for <sup>13</sup>C NMR in DMSO solution.

### Preparation of magnetic Fe<sub>3</sub>O<sub>4</sub> nano particles (MNPs)

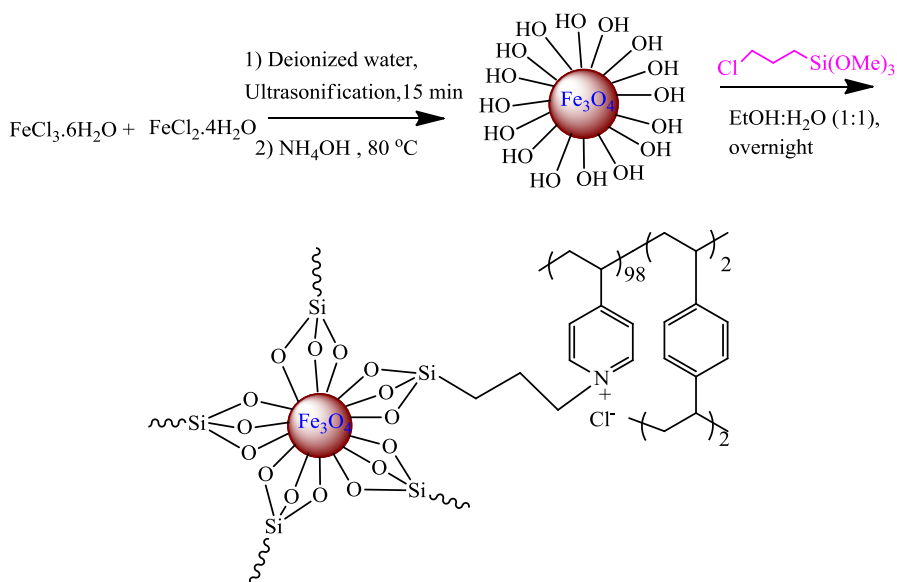
In a typical procedure, 2 mmol FeCl<sub>3</sub>·6H<sub>2</sub>O (1.6 g) and 1 mmol FeCl<sub>2</sub>·4H<sub>2</sub>O (0.8 g) were dissolved in deionized water (0.9 mL) under ultrasound treatment and under N<sub>2</sub> atmosphere for 15 min. Thereafter, under rapid mechanical stirring, 15 mL of dilute aqueous ammonia (NH<sub>4</sub>OH) was added drop-wise into this solution within 30 min. The resulting black precipitate was isolated with external magnet and then washed with distilled water (4 × 5 mL) and finally dried at 80 °C in a vacuum oven.

### Preparation of [P<sub>4</sub>-VP]-Fe<sub>3</sub>O<sub>4</sub>

The synthesized Fe<sub>3</sub>O<sub>4</sub> nanoparticles (2 g) were dispersed in EtOH/H<sub>2</sub>O (1/1, 20 mL) under ultrasonication for 15 min. Then (3-chloropropyl) trimethoxysilane (3.4 g, 16 mmol) was added to this mixture and stirred overnight at 80 °C. Thereafter, [P<sub>4</sub>-VP] 2%DVB (1 g) was added to the resulted mixture and stirred at 80 °C for 20 h. The resulting [P<sub>4</sub>-VP]-Fe<sub>3</sub>O<sub>4</sub> were collected by external magnet, washed three times with ethanol (5 mL) and finally dried at 50 °C in a vacuum oven (Scheme 2).

### General procedure for the synthesis of 4,5-diphenyl-2aryl imidazoles

To the mixture of benzil (1 mmol), aldehydes (1.3 mmol) and ammonium acetate (3.5 mmol), [P<sub>4</sub>-VP]-Fe<sub>3</sub>O<sub>4</sub> (0.1 g) was added and the mixture was stirred at 100 °C under solvent-free conditions for 20–80 min. Progress of the reaction was monitored by TLC (n-hexane/EtOAc, 80/20). After completion, the reaction mixture was dissolved in EtOH (1 mL), and then [P<sub>4</sub>-VP]-Fe<sub>3</sub>O<sub>4</sub> was separated from



**Scheme 2** Preparation of [P<sub>4</sub>-VP]-Fe<sub>3</sub>O<sub>4</sub>

the mixture by using an external magnet. Thereafter, by pouring crushed ice onto the dissolved mixture, the white product was precipitated. Then for further purification, the crude product was recrystallized from EtOH to afford the corresponding 4,5-diphenyl-2-aryl imidazoles in good to high yields (68–99%).

## Results and discussion

[P<sub>4</sub>-VP]-Fe<sub>3</sub>O<sub>4</sub> as a novel magnetic polymeric catalyst was prepared, and in order to investigate its structure, FT-IR, XRD, FESEM and VSM techniques were used. As it is shown in the FT-IR spectra of Fe<sub>3</sub>O<sub>4</sub> MNPs (Fig. 1), the characteristic adsorption of stretching vibration of Fe–O bond appeared at 598 cm<sup>-1</sup> and the stretching vibration of surface OH groups was presented at 3390 cm<sup>-1</sup> (Fig. 1a). A similar characteristic peak of Fe–O bond can be seen at 576 cm<sup>-1</sup> in Fig. 1c, which shifts to a lower value and may be attributed to the location of MNPs in the polymeric structure.

It can be found that compared to Fe<sub>3</sub>O<sub>4</sub>, some new peaks related to polymer was appeared in Fig. 1c at 2924, 2956 (related to CH<sub>2</sub> stretching vibration), 1637, 1513 (assigned to C=N and C=C bond of pyridine ring respectively), 1116 and 1039 cm<sup>-1</sup> (are assigned to the in-plane and out-of-plane rings C–H bending, respectively), also similar adsorption of surface OH groups appeared at 3435 cm<sup>-1</sup>, which, compared to Fig. 1a, its intensity probably is due to the linking of Fe<sub>3</sub>O<sub>4</sub> nanoparticles to [P<sub>4</sub>-VP] 2%DVB. Clearly, there is slight shifting in band peaks of the pyridine ring in Fig. 1c compared to Fig. 1b, which in turn confirmed the location of Fe<sub>3</sub>O<sub>4</sub> nanoparticles in the polymer structure, and the pyridine rings were

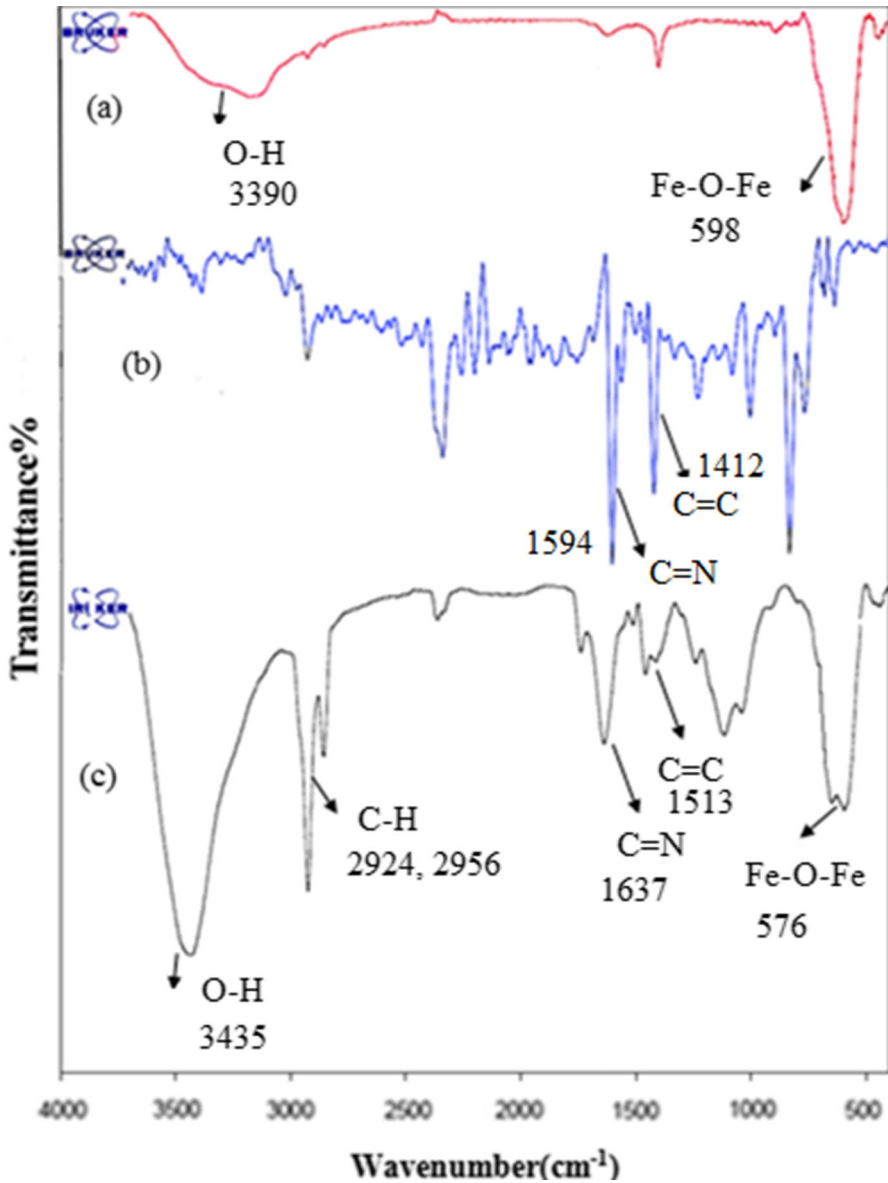


Fig. 1 FT-IR spectrum of **a**  $\text{Fe}_3\text{O}_4$ , **b**  $[\text{P}_4\text{-VP}]2\%\text{DVB}$  and **c**  $[\text{P}_4\text{-VP}]\text{-Fe}_3\text{O}_4$

converted to pyridinium pendent groups. The obtained results are supported by other previously reported of our works in the literature [21, 45].

The XRD-diffraction patterns of the prepared  $[\text{P}_4\text{-VP}]\text{-Fe}_3\text{O}_4$  and  $[\text{P}_4\text{-VP}]2\%\text{DVB}$  are shown in Fig. 2.

As it indicated  $[\text{P}_4\text{-VP}]2\%\text{DVB}$  had amorphous structure that by adding  $\text{Fe}_3\text{O}_4$  nanoparticles, the structure was affected and changed to crystalline form. These

structural changes well confirmed the placement of MNPs in the polymer structure. Nine characteristic peaks were found in the XRD patterns of [P<sub>4</sub>-VP]-Fe<sub>3</sub>O<sub>4</sub> at  $2\theta = 18.71, 30.38, 35.75, 37.12, 43.34, 53.73, 57.23, 63.06, 74.73$ , which correspond to (111), (220), (311), (222), (400), (422), (511), (440), (533) planes, respectively. The position and relative intensities of all peaks match well with standard XRD pattern of Fe<sub>3</sub>O<sub>4</sub> [48] (JCPDS Card No. 00-001-1111) indicating the crystalline cubic spinel structure of Fe<sub>3</sub>O<sub>4</sub> in the [P<sub>4</sub>-VP]-Fe<sub>3</sub>O<sub>4</sub> catalyst. According to the higher intensity of peaks in the (311) plane compared to the other planes, it can be concluded that this is the preferred orientation of Fe<sub>3</sub>O<sub>4</sub> in [P<sub>4</sub>-VP]-Fe<sub>3</sub>O<sub>4</sub>. Debye–Scherrer’s equation [46–49], ( $D = 0.9\lambda/\beta\cos\theta$ , where  $D$  is the average crystalite size,  $\lambda$  is the X-ray wavelength used and is equal to 0.154,  $\beta$  is the angular line width at half maximum intensity [FWHM and is equal to 0.5117 degrees, which should be converted into the length unit by using of  $(\beta \times 2 \times 3.1416)/360$ ], and  $\theta$  is Bragg’s angle in degrees), was used to determine the crystal size of Fe<sub>3</sub>O<sub>4</sub> nanoparticles in [P<sub>4</sub>-VP]-Fe<sub>3</sub>O<sub>4</sub>. The crystal size of the MNPs was found to be 16.34 nm.

Morphology and distribution of Fe<sub>3</sub>O<sub>4</sub> MNPs on the structure of [P<sub>4</sub>-VP] 2%DVB were investigated by FE-SEM, EDX and mapping techniques. According to the FE-SEM images of Fe<sub>3</sub>O<sub>4</sub> MNPs, [P<sub>4</sub>-VP]2%DVB and [P<sub>4</sub>-VP]-Fe<sub>3</sub>O<sub>4</sub>, shown in Fig. 3.

It can be observed that the size of Fe<sub>3</sub>O<sub>4</sub> MNPs and Fe<sub>3</sub>O<sub>4</sub> in the [P<sub>4</sub>-VP]-Fe<sub>3</sub>O<sub>4</sub> are both nanosized and their average sizes are about 26 nm (b and d in Fig. 3, respectively). Furthermore, uniform distribution of Fe<sub>3</sub>O<sub>4</sub> MNPs in the polymeric structure is clearly observed when comparing of c with d in Fig. 3. Differences between FE-SEM images of [P<sub>4</sub>-VP] 2%DVB and [P<sub>4</sub>-VP]-Fe<sub>3</sub>O<sub>4</sub> (shown in Fig. 3 a, c, respectively) proves that Fe<sub>3</sub>O<sub>4</sub> MNPs is added to the surface of polymer and also the surface of polymer is changed after adding Fe<sub>3</sub>O<sub>4</sub> MNPs.

The distribution of the Fe<sub>3</sub>O<sub>4</sub> nanoparticles is also analyzed by elements mapping attached to SEM. It is found that Fe<sub>3</sub>O<sub>4</sub> nanoparticles are, in general, homogeneously dispersed in the polymer. In order to ensure the presence of Fe<sub>3</sub>O<sub>4</sub> MNPs in the polymer structure, EDS analysis was used. It should be noted that EDS analysis is an elemental analysis, and according to the weight percentages and observation of

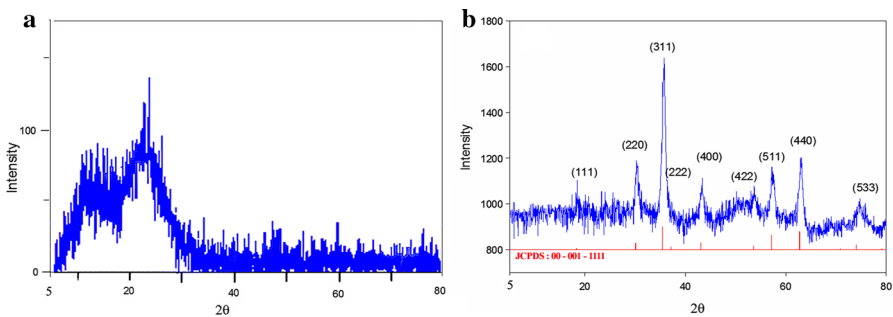


**Fig. 2** XRD patterns of **a** [P<sub>4</sub>-VP]2% DVB and **b** [P<sub>4</sub>-VP]-Fe<sub>3</sub>O<sub>4</sub>

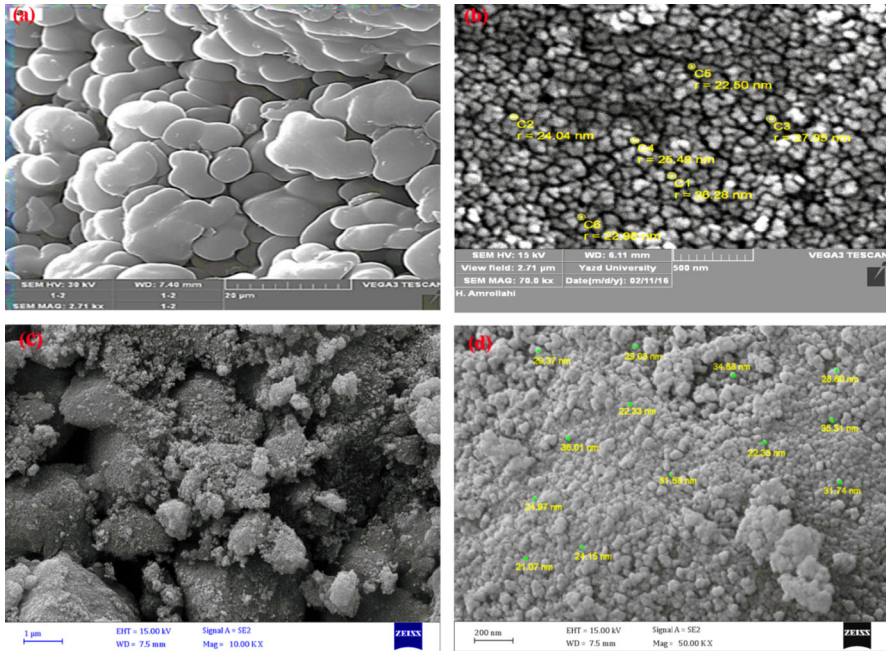


**Fig. 3** FE-SEM images of **a** [P<sub>4</sub>-VP] 2%DVB, **b** Fe<sub>3</sub>O<sub>4</sub> MNPs and **c** [P<sub>4</sub>-VP]-Fe<sub>3</sub>O<sub>4</sub> with magnification of 10 kx and **d** [P<sub>4</sub>-VP]-Fe<sub>3</sub>O<sub>4</sub> with a magnification of 50 kx

Fe and O peaks, it can be concluded that Fe<sub>3</sub>O<sub>4</sub> MNPs is located in the polymer structure (Fig. 4).

Also, the results of elements mapping analysis in Fig. 5 show the relatively uniform distribution of Fe<sub>3</sub>O<sub>4</sub> nanoparticles in the polymer structure.

The magnetization curves for Fe<sub>3</sub>O<sub>4</sub> nanoparticles and [P<sub>4</sub>-VP]-Fe<sub>3</sub>O<sub>4</sub> are shown in Fig. 6.

Magnetization (M) versus applied magnetic field (H) curve measurements of the samples indicate a saturation magnetization values (M<sub>s</sub>) of 62.76 and 40 emu g<sup>-1</sup> for Fe<sub>3</sub>O<sub>4</sub> and [P<sub>4</sub>-VP]-Fe<sub>3</sub>O<sub>4</sub>, respectively. Figure 6 shows that there is no hysteresis loop, H<sub>c</sub> = 0 Oe, which indicates the super paramagnetic nature of these samples. Superparamagnetic nanocrystals are believed to be promising for wide applications in engineering, such as drug delivery, bioseparation and magnetic resonance imaging [50–52].

### Catalyst activity

Catalytic activity of [P<sub>4</sub>-VP]-Fe<sub>3</sub>O<sub>4</sub> was studied in the synthesis of imidazole derivatives in one-pot three-component reaction of benzil, ammonium acetate and aldehydes. First, for optimization of the reaction conditions, the reaction of benzil (1 mmol), ammonium acetate (3.5 mmol) and benzaldehyde (1.3 mmol) in the presence of various amount of [P<sub>4</sub>-VP]-Fe<sub>3</sub>O<sub>4</sub> under solvent-free conditions at 100 °C was investigated (as the model reaction) (Table 1, entries 1–4).

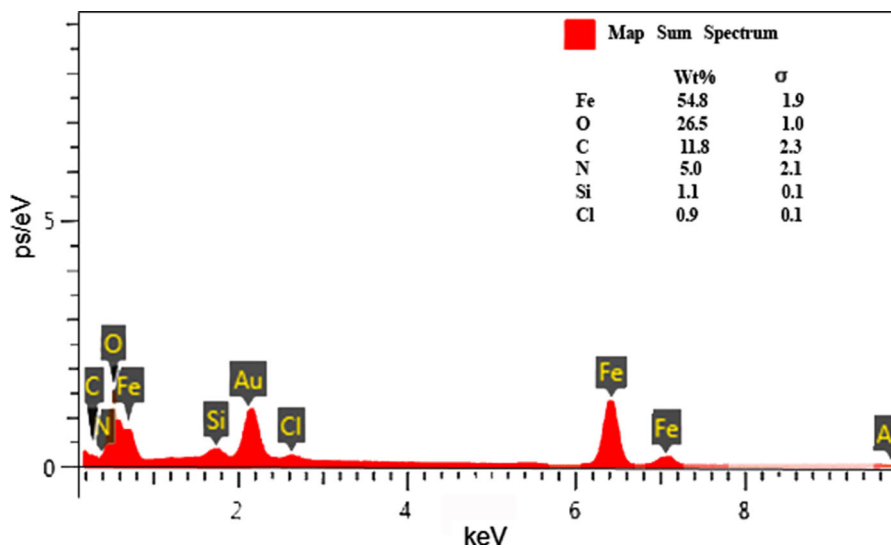


Fig. 4 EDS analysis of [P<sub>4</sub>-VP]-Fe<sub>3</sub>O<sub>4</sub>

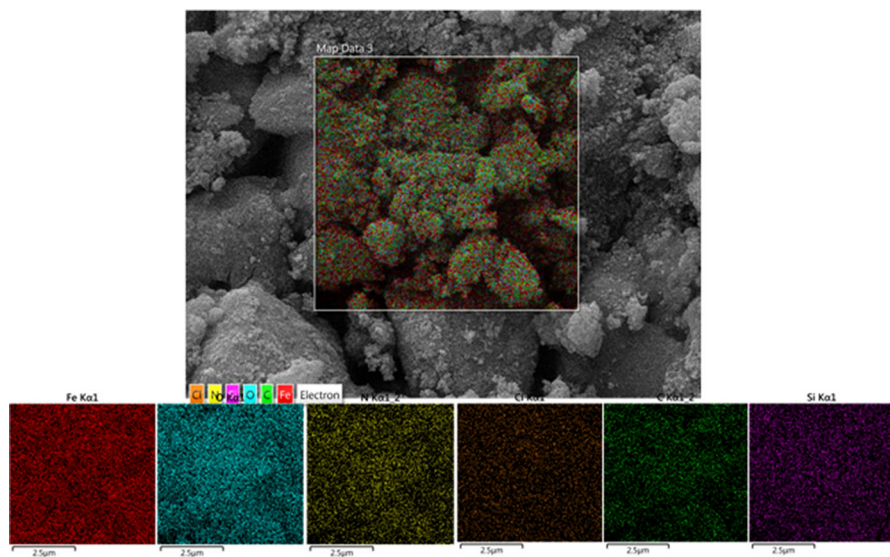
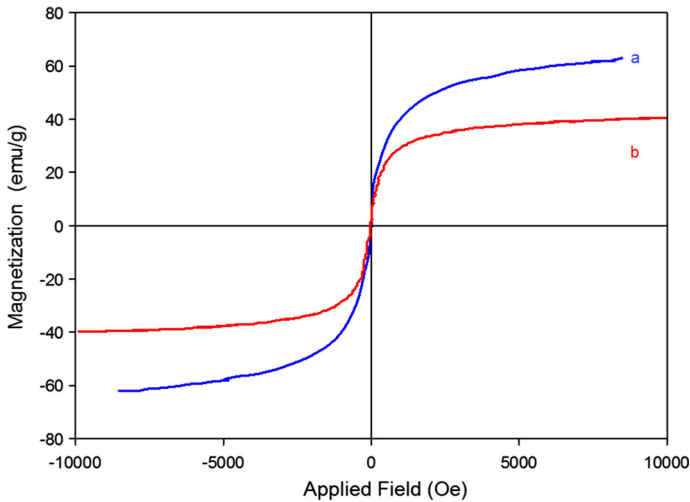


Fig. 5 Elements mapping analysis of [P<sub>4</sub>-VP]-Fe<sub>3</sub>O<sub>4</sub>

As it is clear from Table 1 (entry 3) and according to the reaction time, yield of product and the use of a minimum amount of catalyst, 100 (mg) was selected as the best amount of the catalyst. In the next investigation, effect of temperature was studied and the model reaction was carried out at different temperatures under solvent-free conditions in the presence of 100 mg of the catalyst (Table 1, entries 5–8). The results showed that highest yield in the shortest time was achieved at



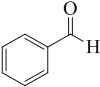
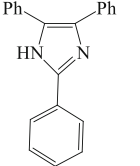
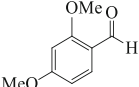
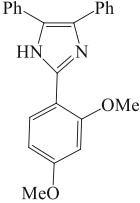
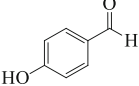
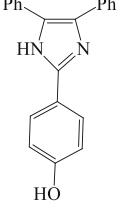
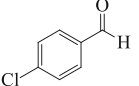
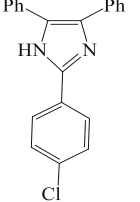
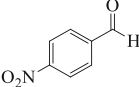
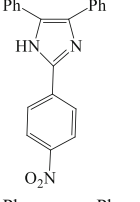
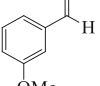
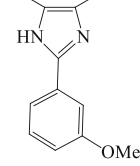
**Fig. 6** Vibrating sample magnetometry (VSM) curves for (a)  $\text{Fe}_3\text{O}_4$  MNPs and (b)  $[\text{P}_4\text{-VP}]\text{-Fe}_3\text{O}_4$  MNPs

**Table 1** Optimization of the reaction conditions in the reaction of benzil (1 mmol), ammonium acetate (3.5 mmol) and benzaldehyde (1.3 mmol) under solvent-free conditions

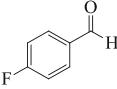
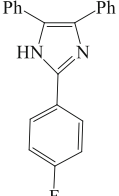
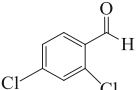
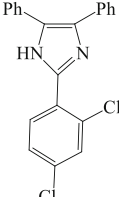
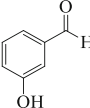
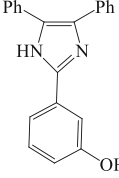
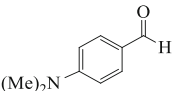
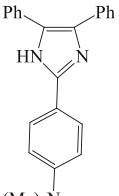
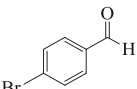
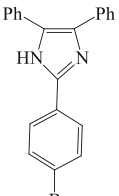
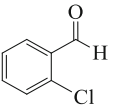
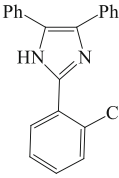
Entry	Catalyst (mg)	Solvent	Temperature ( $^{\circ}\text{C}$ )	Time (min)	Yield (%)
1	200	Solvent-free	100	80	85
2	150	Solvent-free	100	55	77
3	100	Solvent-free	100	35	98
4	75	Solvent-free	100	105	71
5	100	Solvent-free	110	35	98
6	100	Solvent-free	90	180	80
7	100	Solvent-free	80	240	79
8	100	Solvent-free	r.t.	24 h	60% progress
9	100	EtOH	80	270	80
10	100	DMF	120	12 h	65
11	100	$\text{CH}_3\text{CN}$	82	24 h	40% progress
12	100	$\text{CH}_2\text{Cl}_2$	40	24 h	10% progress
13	$\text{Fe}_3\text{O}_4$ (46 mg)	Solvent-free	100	35	91
14	Without linker (100 mg)	Solvent-free	100	48	80

100  $^{\circ}\text{C}$  (Table 1, entry 3). By performing the model reaction in various solvents (Table 1, entries 7–10) and comparing the results with the solvent-free condition it was found that the solvent-free condition led to the best results. In the next step, we investigated the effect of linker on the catalyst reactivity. For this purpose, the model reaction was done in the presence of  $[\text{P}_4\text{-VP}]\text{-Fe}_3\text{O}_4$  synthesized without using a linker (the mixture of  $\text{Fe}_3\text{O}_4$ , 2 g. and  $[\text{P}_4\text{-VP}]$  2%DVB, 1 g. in 20 mL of

**Table 2** Synthesis of imidazole derivatives from the reaction of benzil (1 mmol), ammonium acetate (3.5 mmol) and benzaldehydes (1.3 mmol) in the presence of 100 mg of [P<sub>4</sub>-VP]-Fe<sub>3</sub>O<sub>4</sub> at 100 °C under solvent-free conditions

Entry	Aldehyde	Product	Time (min)	Yield (%) <sup>a</sup>	M.P.	
					Found	Reported Ref.
1			35	98	278–279	274–276 [40]
2			40	91	255–256	250–252 [55]
3			40	99	266–267	268–270 [53]
4			50	87	262–264	261–262 [40]
5			240	68	238–239	238–240 [42]
6			80	85	260–262	258–260 [43]

**Table 2** continued

Entry	Aldehyde	Product	Time (min)	Yield (%) <sup>a</sup>	M.P.	
					Found	Reported Ref.
7			70	92	258–259	250–251 [56]
8			75	87	173–175	174–175 [40]
9			65	80	260–262	260–261 [43]
10			50	79	254–255	256–258 [54]
11			70	90	260–262	260–262 [41]
12			60	89	193–195	196–198 [42]

<sup>a</sup>Isolated yield

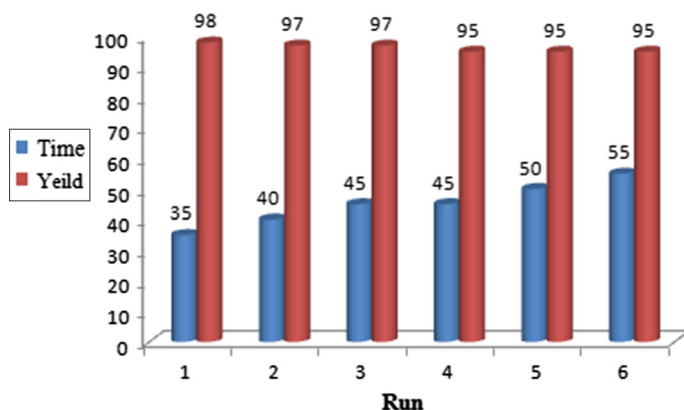


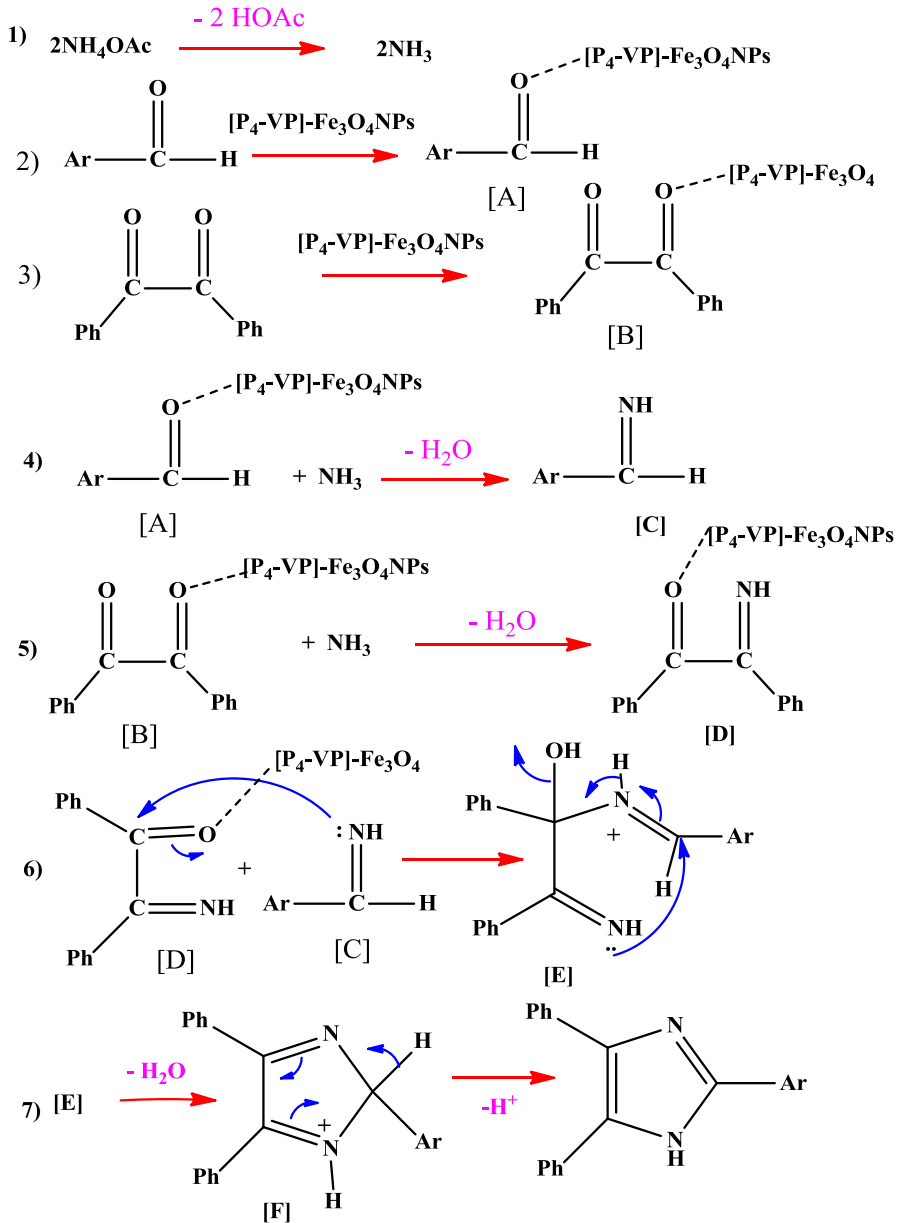
Fig. 7 Reusability of the catalyst in the model reaction

EtOH/H<sub>2</sub>O, 1/1, was stirred at 80 °C for 20 h.) and the results showed that this reaction was done in a longer reaction time. We also studied the reaction in the presence of Fe<sub>3</sub>O<sub>4</sub> nanoparticles and by comparing it with the result of doing the same reaction in the presence of [P<sub>4</sub>-VP]-Fe<sub>3</sub>O<sub>4</sub>, it became clear that in the same time a higher yield was obtained in the presence of [P<sub>4</sub>-VP]-Fe<sub>3</sub>O<sub>4</sub> (entry 3 and 11). After optimization of the reaction conditions imidazole derivatives were synthesized from the reaction of benzil (1 mmol), ammonium acetate (3.5 mmol) and benzaldehydes (1.3 mmol) in the presence of 100 mg of [P<sub>4</sub>-VP]-Fe<sub>3</sub>O<sub>4</sub> at 100 °C under solvent-free conditions with good to high yields (Table 2).

It is necessary to note that the reaction was carried out with 1 and 1.2 mmol of aldehydes, but it led to byproducts and non-completion of the reaction.

Finally, to investigate reusability of the catalyst, the recovered catalyst from the model reaction was washed with EtOH, dried at 80 °C for 4 h and used six times in the same reaction conditions without significant loss of catalytic activity. The results of this study are shown in Fig. 7. It can be seen that after six times reusing of the catalyst in the same reaction and under identical conditions, a little decreasing in the yield of product was found, which indicates that no decomposition of the polymer and low leaching of Fe<sub>3</sub>O<sub>4</sub> were observed throughout the reaction mixture.

It can be understood from similar studies reported in the literature [43] that the plausible mechanism for the formation of 2,4,5 tri-substituted imidazoles is shown in Scheme 3. In the first step, ammonia is formed by decomposition of ammonium acetate by heating. On the other hand, aldehyde and 1,2-diketone are activated by [P<sub>4</sub>-VP]-Fe<sub>3</sub>O<sub>4</sub>NPs to afford intermediates [A] and [B], respectively. Then imine intermediates [C] and [D] are produced by nucleophilic addition of ammonia to activated aldehyde [A] and activated 1,2-diketone [B], respectively. Imine intermediate [C], condenses further with the carbonyl carbon of 1,2-diketone imine [D] to form carbocation [E]. Carbocation [E] followed by attack of the nitrogen atom of imine to the carbon atom of the iminium-positive center affords the cyclization with dehydration to produce *iso*-imidazole [F], which rearranges via [1, 5] sigmatropic hydrogen shift to the required imidazole (Scheme 3).



**Scheme 3** The plausible mechanism for the formation of 2,4,5 tri-substituted imidazoles

Finally, we compared our work with other works. As it is clear from Table 3, according to the reaction time, yields of the products and in some works in respect to the temperature of the reaction our work is comparable.

**Table 3** Comparison of the yield, time and reaction conditions for the model reaction with other multicomponent reported methods

Entry	Reaction conditions	Time (min)	Yield (%) <sup>a</sup>	Ref
1	AMPS-co-AA (30 mg), solvent-free, 110 °C	25	92	[55]
2	Nano SiO <sub>2</sub> -supported FHS (40 mg), solvent-free, 110 °C	30	90	[42]
3	[C <sub>4</sub> (mim) <sub>2</sub> ](FeCl <sub>4</sub> ) <sub>2</sub> , solvent-free, 100 °C	50	90	[57]
5	Monmorillonite (25 mg), EtOH, reflux	90	70	[58]
6	Zeolite (25 mg), EtOH, reflux	60	80	[58]
7	Nano crystalline SZ (25 mg) EtOH, reflux	45	87	[58]
8	DEP (1 mol), US, r.t	40	95	[53]
9	Fe <sub>3</sub> O <sub>4</sub> (5 mol %), EtOH, reflux, r.t	120	90	[43]
10	Catalyst-free and solvent-free, 130 °C	180	80	[59]
11	[P <sub>4</sub> -VP]-Fe <sub>3</sub> O <sub>4</sub> (100 mg), solvent-free, 100 °C	35(min)	98	[A] <sup>b</sup>

AMPS acrylamido-2-methyl-1-propane sulphonic acid, AA Acrylic acid, FHS Feric hydrogen sulfate, SZ solfated zirconia, DEP diethyl bromophosphate

<sup>a</sup>Yields refer to isolated products

<sup>b</sup>A = Present method (Table 1, entry 3)

## Conclusion

A simple and green protocol for the synthesis of imidazole derivatives using [P<sub>4</sub>-VP]-Fe<sub>3</sub>O<sub>4</sub> as a magnetic and efficient catalyst was reported in our work. The catalyst is insole in the reaction medium and magnetic property and, consequently, is easily recovered by using an external magnet. The introduced catalyst can promote yields and reaction times in comparison with many repeated methods with very low leaching amounts of supported catalyst into the reaction mixture. Moreover, high yields of products, short reaction times, ease of work-up and clean procedure makes the present method a useful and important addition to the previous methodologies. In addition, there is current research and general interest in heterogeneous systems because such systems have importance in industry and in developing technologies. Recycling experiments show that [P<sub>4</sub>-VP]-Fe<sub>3</sub>O<sub>4</sub> can be recovered and reused several times without significant loss of their activity.

**Acknowledgements** The authors thank the University of Yazd for the support of this work.

## References

1. A.L. Morel, S.I. Nikitenko, K. Gionnet, A. Wattiaux, J. LaiKee-Him, C. Labrugere, B. Chevalier, G. Deleris, C. Petibois, A. Brisson, M. Simonoff, *J. Am. Chem. Soc.* **2**, 847 (2008)
2. Y. Weia, B. Hanb, X. Hua, Y. Linc, X. Wangd, X. Denga, *Procedia Eng.* **27**, 632 (2012)
3. M. Abdel Aleem, A. El-Remaily, A.M. Abu-Dief, R.M. El-Khatib, *Appl. Organomet. Chem.* **30**, 1022 (2016)
4. D. Astruc, *Nanoparticles and Catalysis* (Wiley, New York, 2008)
5. Y. Xia, H. Yang, C.T. Cambell, *Acc. Chem. Res.* **46**, 1671 (2013)

6. L. Shen, P.E. Laibinis, T.A. Hatton, *Langmuir* **15**, 447 (1999)
7. A. Jordan, R. Scholz, P. Wust, H. Föhling, R. Felix, J. Magn. Magn. Mater. **201**, 413 (1999)
8. J.Q. Cao, Y.X. Wang, J.F. Yu, J.Y. Xia, C.F. Zhang, D.Z. Yin, U.O. Hafeli, J. Magn. Magn. Mater. **277**, 165 (2004)
9. A. Jordan, R. Scholz, P. Wust, H. Schirra, T. Schiestel, H. Schmidt, R. Felix, J. Magn. Magn. Mater. **194**, 185 (1999)
10. Q. Li, Y.M. Xuan, J. Wang, *Exp. Therm. Fluid. Sci.* **30**, 109 (2005)
11. S. Sun, H. Zeng, *J. Am. Chem. Soc.* **124**, 8204 (2002)
12. L. Liz, M.A. Lopez Quintela, J. Mira, J. Rivas, *J. Mater. Sci.* **29**, 3797 (1994)
13. H.S. Lee, W.O. Lee, *J. Appl. Phys.* **85**, 5231 (1999)
14. Z.L. Liu, X. Wang, K.L. Yao, G.H. Du, Q.H. Lu, Z.H. Ding, J. Tao, Q. Ning, X.P. Luo, D.Y. Tian, D. Xi, *J. Mater. Sci.* **39**, 2633 (2004)
15. Y.J. Lee, J.W. Lee, C.J. Bae, J.G. Park, H.J. Noh, J.H. Park, T. Hyeon, *Adv. Func. Mater.* **15**, 503 (2005)
16. A.B. Chin, I.I. Yaacob, *J. Mater. Process Tech.* **191**, 235 (2007)
17. M. Sasmita, P. Nabakumar, M. Samrat, K.G. Sudip, P. Panchanan, *J. Mater. Sci.* **42**, 7566 (2007)
18. Y. Zhang, S.N. Wang, S. Ma, J.J. Guan, D. Li, X.D. Zhang, Z.D. Zhang, *J. Biomed. Mater. Res.* **85A**, 840 (2008)
19. M.A.K. Zarchi, S.S.A. Darbandizadeh Mohammad Abadi, *New J. Chem.* **41**, 10397 (2017)
20. M.A. Karimi Zarchi, R. Banihashemi, *J. Sulfur Chem.* **37**, 282 (2016)
21. M.A. Karimi Zarchi, F. Nazem, *J. Iran. Chem. Soc.* **11**, 1731 (2014)
22. M.A. Karimi Zarchi, N. Ebrahimi, *Phosphorus Sulfur.* **187**, 1226 (2012)
23. M.A. Karimi Zarchi, Z. Mousavi, *J. Polym. Res.* **21**, 330 (2014)
24. M.A. Karimi Zarchi, A. Tabatabaei Bafghi, *J. Sulfur Chem.* **36**, 403 (2015)
25. M.A. Karimi Zarchi, R.Z. Escandari, *J. Appl. Polym. Sci.* **121**, 1916 (2011)
26. A.R. Pourali, S. Ghayeni, F. Afghahi, *Bull. Korean Chem. Soc.* **34**, 1741 (2013)
27. J.W. Black, G.J. Durant, J.C. Emmett, C.R. Ganellin, *Nature* **248**, 65 (1974)
28. U. Ucucu, N.G. Karaburun, I. Iskdag, *Farmaco* **56**, 285 (2001)
29. J.A. Murry, *Drug Discov. Dev.* **6**, 945 (2003)
30. M. Abdel Aleem, A.A. El-Remaily, A.M. Abu-Dief, *Tetrahedron* **71**, 2579 (2015)
31. S.R. Sarkar, C. Mukhopadhyay, *Eur. J. Org. Chem.* **6**, 1246 (2015)
32. H. Sharghi, M. Aberi, M.M. Doroodmand, *Mol. Divers.* **19**, 77 (2015)
33. H. Zang, Q. Su, Y. Mo, B.W. Cheng, S. Jun, *Ultrason. Sonochem.* **17**, 749 (2010)
34. D. Kumar, K.R.J. Thomas, *J. Photochem. Photobiol.* **218**, 162 (2011)
35. V. Srot, M. Gec, P.A. Aken, J. Jeon, M. Ceh, *Micron* **62**, 37 (2014)
36. H. Debus, *Annal. Chemi. Pharm.* **107**, 199 (1858)
37. A.A. Marzouk, A.M. Abu-Dief, A.A. Abdelhamid, *Appl. Organomet. Chem.* **32**, e3794 (2018)
38. H.V. Chavan, D.K. Narale, *C. R. Chim.* **17**, 980 (2014)
39. B. Maleki, H. Eshghi, A. Khojastehnezhad, R. Tayebbe, S.S. Ashrafi, G. Esmailian, F.K. Moeinpour, *R.S.C. Adv.* **5**, 64850 (2015)
40. N.V. Gandhare, R.G. Chaudhary, V.P. Meshram, J.A. Tanna, S. Lade, M.P. Gharpureand, H.D. Juneja, *J. Chin. Adv. Mater. Soc.* **3**, 270 (2015)
41. P.D. Sanasi, D. Santhipria, Y. Ramesh, M. Ravikumar, B. Swathi, K. Jaya Rao, *J. Chem. Sci.* **126**, 1715 (2014)
42. M. Bakavoli, H. Eshghi, A. Mohammadi, H. Moradi, J. Ebrahimi, *Iran J. Catal.* **5**, 237 (2015)
43. J. Safari, Z. Zarnegar, *Iran. J. Catal.* **2**, 121 (2012)
44. G. Sharma, Y. Jyothi, P. Lakshmi, *Synth. Commun.* **36**, 2991 (2006)
45. M.A. Karimi Zarchi, A. Tarabsaz, *Phosphorus Sulfur.* **190**, 550 (2015)
46. L.H. Abdel-Rahman, A.M. Abu-Dief, R.M. El-Khatib, Sh.M. Abdel-Fatah, *J. Photochem. Photobiol. B Biol.* **162**, 298 (2016)
47. A.M. Abu-Dief, W.S. Mohamed, *Mater. Res. Express* **4**, 035039 (2017)
48. E.M.M. Ibrahim, A.M. Abu-Dief, A. Elshafaie, A.M. Ahmed, *Mater. Chem. Phys.* **192**, 41 (2017)
49. W.S. Mohamed, A.M. Abu-Dief, *J. Phys. Chem. Solids* **116**, 375 (2018)
50. A.M. Abu-Dief, M.S.M. Abdelbaky, D. Martínez-Blanco, Z. Amghouz, S. García-Granda, *Mater. Chem. Phys.* **174**, 164 (2016)
51. E.M.M. Ibrahim, L.H. Abdel-Rahman, A.M. Abu-Dief, A. Elshafaie, S. Kamel Hamdan, A.M. Ahmed, *Mater. Res. Bull.* **99**, 103 (2018)
52. C. Hu, Z. Gao, X. Yang, *J. Magn. Magn. Mater.* **320**, 70 (2008)

53. D. Nagargoje, P. Mandhane, S. Shingote, P. Badadhe, C. Gill, *Ultrason. Sonochem.* **19**, 94 (2012)
54. H.R. Shaterian, M. Ranjbar, K. Azizi, *Chin. J. Chem.* **29**, 1635 (2011)
55. A. Mohammadi, H. Keshvari, R. Sandaroots, H. Rouhi, *J. Chem. Sci.* **124**, 717 (2012)
56. C. Yu, M. Lei, W. Su, Y. Xie, *Synth. Commun.* **37**, 3301 (2007)
57. B. Mombani Godajdar, A.R. Kiasat, *Iran. J. Catal.* **3**, 229 (2013)
58. A. Teimouri, A.N. Chermahini, *J. Mol. Catal.* **346**, 39 (2011)
59. S. Samanta, S. Sarkar, R. Pal, K.A. Maleki, *Org. Chem. Int.* **2013**, 1 (2013)

## Affiliations

Zeinab Hamidi<sup>1</sup>  · Mohammad Ali Karimi Zarchi<sup>1</sup>

✉ Mohammad Ali Karimi Zarchi  
makarimi@yazd.ac.ir

<sup>1</sup> Department of Chemistry, College of Science, Yazd University,  
P.O. Box 89195-741, Yazd 8915813149, Iran